J. Fluid Mech. (1986), *vol.* 173. *pp.* 501–518
Printed in Great Britain

Experiments with baroclinic vortex pairs in a rotating fluid

By R. W. GRIFFITHS

Research School of Earth Sciences, The Australian National University, G.P.O. Box 4, Canberra 2601, Australia

AND E. J. HOPFINGER

Institut de Mécanique, Laboratoire Associé au CNRS, Université de Grenoble, B.P. 68, 38402 St. Martin d'Hères, France

(Received 25 March 1986)

When vortices are generated in one layer of a rotating, two-layer density stratification, the velocity field of each vortex is strongly baroclinic within a distance of order one Rossby radius from its centre. In this system there are two classes of vortex pairs: those pairs (consisting of vortices of opposite signs) for which the vortices are in the same layer, and those for which the vortices are in opposite layers. We pay particular attention to a laboratory demonstration of the properties of the latter class. These vortex pairs have the ability to transport density (or heat) in the horizontal, and provide a means for describing the release of potential energy by baroclinic instability. We also observe that interactions of real vortices and real vortex pairs differ from those computed for point vortices.

1. Introduction

Geostrophic vortices in stratified oceans and atmospheres are complicated structures which undergo even more complex interactions with each other. Their structure and interactions are influenced by, among other factors, the internal Rossby radius for the fluid, a horizontal lengthscale which becomes a characteristic radius for the vortex flow. The influence of one baroclinic vortex on another must also depend upon the vertical distribution of horizontal velocity induced by each vortex, distributions that are determined by the forcing or mechanism by which the vortices are generated. This generation mechanism is most commonly the growth of unstable baroclinic waves as they release potential energy from rotating, stratified shear flows. The baroclinic vortices present local maxima in potential energy, but relative motions of two or more vortices can decrease (or increase) the total potential energy of the flow. Interactions, which at this stage are little investigated and poorly understood, between such vortices influence the fate of individual ocean eddies and atmospheric vortices, and make up the statistical properties of geostrophic turbulence.

Gryanik (1983) and Hogg & Stommel (1985*a*) present a much simplified but useful model of baroclinic vortices. The model assumes a two-layer density stratification and represents each vortex by a point vortex (a delta function in potential vorticity) lying wholly within one layer. Such a vortex induces an azimuthal flow in its own layer. However, this flow also causes vertical displacements of the interface in order to maintain geostrophic balance, and thereby creates relative vorticity by stretching

or compression of fluid columns in the opposite layer. The two-layer flow is strongly baroclinic within a distance of the order of the Rossby radius and becomes independent of depth at large distances. Thus interaction between two vortices depends on whether they are in the same or opposite layers when they are separated by less than several Rossby radii.

One of the most significant of vortex interactions is that between two vortices of opposite sign. As in the more familiar case of a non-rotating and unstratified fluid, two such vortices in a rotating flow form a propagating vortex pair. However, in the two-layer case there are two classes of vortex pairs. In one class the vortices of opposite sign are in the same layer. These vortices influence each other more strongly when closer together, and therefore the pair propagates more rapidly. Through the need to maintain geostrophic balance the two vortices of opposite sign displace the density interface in opposite directions, so that if their strengths are equal the pair effects no net transport of density. The second class of vortex pairs consists of pairs with vortices of opposite signs in opposite layers. In this class, the translation speed is a maximum when the horizontal separation of vortices is close to one Rossby radius. Furthermore, both vortices displace the interface in the same direction, and translation involves a net horizontal transport of density. Thus an anticyclone in the top layer and a neighbouring cyclone in the bottom layer, for example, both cause the density interface to dome downwards, and the pair effects a net transport of less-dense top-layer water in the direction of its translation. Since a vortex pair is a coherent structure, and because density differences in geophysics are most often produced by temperature differences, Hogg & Stommel (1985*a*) named this heat-transporting baroclinic pair a 'heton'. We continue the use of the term 'heton' as it provides a convenient shorthand for the special vortex pair described above.

In order to further elucidate the fundamental properties of baroclinic vortices and the consequences of their interactions, Hogg & Stommel (1985*a*) and Young (1985) computed the paths of four point vortices as they underwent interactions in a number of situations. Of special interest here are the interactions of two hetons. The result of greatest significance is that the velocity shears across the interface cause hetons to tear each other apart if they are separated by less than a Rossby radius, while the barotropic component of the velocity field causes hetons to repel each other if they are separated by a larger distance. The model was extended to compute the rate of spread of a cloud consisting of a very large number of hetons (Hogg & Stommel 1985*b*), and the prediction compared with measurements of the rate of spread of a large patch of less-dense water in a rotating tank (Griffiths & Hopfinger 1984). Despite a good functional agreement, the computed rate of spreading was much greater than that measured.

In this paper we report observations of the interactions of real baroclinic vortices in a laboratory tank. Each vortex was initially generated by a source or a sink in one layer of a two-layer stratification. Vortex pairs of the heton type were produced and, in general, interacted with other hetons as predicted by the point-vortex model. The importance of the Rossby radius was clearly demonstrated. However, after some time, particularly when two vortices of the same sign and in the same layer came close together, the vortex paths deviated from the ideal computed paths, and two vortices were often observed to coalesce. These deviations are attributed to the presence of a core of finite radius, having different potential vorticity, in each real vortex. Section 2 summarizes the results of the two-layer point-vortex model. In §3 we show that the structure of laboratory vortices produced by sources and sinks is satisfactorily described by the point-vortex model, so long as we remain at radii

much greater than that of a finite central core. In §4 we use these vortices to demonstrate the nature of vortex interactions.

2. A quasi-geostrophic point-vortex model

2.1. *Formulation of the model*

A simple model which enables us to compute the consequences of interactions between vortices in a two-layer, rotating flow is that in which each vortex is replaced by a delta function in potential vorticity in one of the two layers, and in which the flow satisfies the quasi-geostrophic potential-vorticity equation.

Each layer is taken to be of uniform density and of depth H. There is a density step $\Delta\rho$ across the interface between layers, the effect of which is wholly contained in the reduced gravity $g' = g\Delta\rho/\rho$. The presence of both buoyancy and Coriolis forces leads to the only horizontal lengthscale for the flow: the Rossby radius of deformation $\lambda = (g'H)^{\frac{1}{2}}/f$, where $f\ (= 2\Omega)$ is the Coriolis parameter. The motion induced by a single point vortex of strength $2\pi s$ is given by the potential-vorticity equations.

$$\left.\begin{aligned} \nabla^2\psi_{\mathrm{a}} - \tfrac{1}{2}\lambda^{-2}(\psi_{\mathrm{a}} - \psi_{\mathrm{b}}) &= 2\pi s\delta(\boldsymbol{x}), \\ \nabla^2\psi_{\mathrm{b}} + \tfrac{1}{2}\lambda^{-2}(\psi_{\mathrm{a}} - \psi_{\mathrm{b}}) &= 0, \end{aligned}\right\} \tag{1}$$

where ψ is a stream function and subscripts a and b refer to the upper and lower layer respectively. The vortex intensity s is positive for a cyclone and negative for an anticyclone. It has been assumed that both layers have the same uniform potential vorticity $\pi = f/H$ except for the delta function in the upper layer. Thus the right-hand side, $\pi H - f$, of the potential-vorticity equation (see Pedlosky 1979) becomes as shown in (1). Velocity components in the upper layer are $u_{\mathrm{a}} = -\psi_{\mathrm{a}y}$ and $v_{\mathrm{a}} = \psi_{\mathrm{a}x}$, with similar expressions for the lower layer. In polar coordinates centred on the vortex the solution to (1) is

$$\left.\begin{aligned} \psi_{\mathrm{a}} &= \tfrac{1}{2}s\left[\ln r - K_0\left(\frac{r}{\lambda}\right)\right], \\ \psi_{\mathrm{b}} &= \tfrac{1}{2}s\left[\ln r + K_0\left(\frac{r}{\lambda}\right)\right], \end{aligned}\right\} \tag{2}$$

and azimuthal velocities are

$$\left.\begin{aligned} v_{\mathrm{a}} &= \frac{1}{2}\frac{s}{r}\left[1 - \frac{r}{\lambda}K_1\left(\frac{r}{\lambda}\right)\right], \\ v_{\mathrm{b}} &= \frac{1}{2}\frac{s}{r}\left[1 - \frac{r}{\lambda}K_1\left(\frac{r}{\lambda}\right)\right]. \end{aligned}\right\} \tag{3}$$

At $r \gg \lambda$, velocities in both layers approach the common form $v = \frac{1}{2}s/r$ and there is no shear across the density interface. Thus the flow at large distances is barotropic (independent of depth), just as it would be at all values of r if the fluid was unstratified (the limit $\lambda \to 0$). At distances comparable with the Rossby radius the velocity in the layer containing the vortex increases with decreasing radius more rapidly than in a barotropic vortex. A baroclinic vortex therefore induces larger velocities within a few Rossby radii than does a barotropic vortex of the same intensity s. The velocity in the opposite layer, however, becomes smaller than that for an unstratified vortex and $v_{\mathrm{b}} = 0$ at $r = 0$. In other words, the induced flow in the two-layer case is strongly baroclinic within two or three Rossby radii, there being

large shears across the interface within this region. (These velocity profiles are compared with laboratory measurements in §3.)

Interactions of a number of point vortices involve simply the advection of each vortex centre by all the other vortices present in the fluid. When vortices are separated by horizontal distances less than a few Rossby radii, the advection of one vortex by the other becomes dependent upon whether they are in the same or opposite layers. Thus, in rectangular coordinates, the ith vortex moves with the velocities

$$\left.\begin{aligned} \dot{x}_i &= -\sum_{j\neq i} \tfrac{1}{2}s_j\left(\frac{y_i-y_j}{r_{ij}^2}\right)\left[1+(-1)^{k_{ij}}\frac{r_{ij}}{\lambda}K_1\left(\frac{r_{ij}}{\lambda}\right)\right], \\ \dot{y}_i &= -\sum_{j\neq i} \tfrac{1}{2}s_j\left(\frac{x_i-x_j}{r_{ij}^2}\right)\left[1+(-1)^{k_{ij}}\frac{r_{ij}}{\lambda}K_1\left(\frac{r_{ij}}{\lambda}\right)\right], \end{aligned}\right\} \tag{4}$$

where $r_{ij}^2 = (x_i-x_j)^2+(y_i-y_j)^2$, and $k_{ij} = 2$ if vortices i and j are in the same layer, $k_{ij} = 1$ if vortices are in opposite layers. If the ith and jth vortices are separated by a distance $r_{ij} \gg \lambda$, their influence on each other is the same as it would be if there were no stratification. However, if $r_{ij} < \lambda$ the two vortices will cause each other to move more strongly if they are also in the same layer, and more slowly if they are in opposite layers.

2.2. *Vortex pairs*

Thus, when considering just two baroclinic vortices in an otherwise stationary fluid, both their signs and their layers are of significance to their behaviour. Two vortices in the same layer and a distance d apart move in circular paths about their common centre of vorticity with angular velocity

$$\omega = \tfrac{1}{2}d^{-2}(s_1+s_2)\left[1+\frac{d}{\lambda}K_1\left(\frac{d}{\lambda}\right)\right]. \tag{5}$$

If these vortices have equal and opposite strengths, $s_1+s_2 = 0$ and their centre of vorticity lies at infinity. The pair translates in a straight line at a speed

$$c = \tfrac{1}{2}d^{-1}s\left[1+\frac{d}{\lambda}K_1\left(\frac{d}{\lambda}\right)\right]. \tag{6}$$

For $d \gg \lambda$, these vortices behave as a barotropic vortex pair.

On the other hand, two vortices in opposite layers cycle about their centre of vorticity with angular velocity

$$\omega = \tfrac{1}{2}d^{-2}(s_1+s_2)\left[1-\frac{d}{\lambda}K_1\left(\frac{d}{\lambda}\right)\right] \tag{7}$$

or, if $s_1+s_2 = 0$, propagate with a speed

$$c = \tfrac{1}{2}d^{-1}s\left[1-\frac{d}{\lambda}K_1\left(\frac{d}{\lambda}\right)\right]. \tag{8}$$

In this case the translation speed c vanishes for $d/\lambda \to 0$, passes through a very flat maximum (for fixed λ) of $c = 0.22\ s/d$ at $d/\lambda = 1.1$, and approaches the barotropic form $c = \frac{1}{2}s/d$ for $d/\lambda \to \infty$. Members of the class of vortex pairs consisting of vortices of opposite sign in opposite layers were termed 'hetons' by Hogg & Stommel (1985*a*) because of their ability to transport a net amount of density (or heat). Both vortices composing a heton displace the density interface in the same direction and the pair contains a greater potential energy than would the two vortices if separated by a large distance. Translation of a heton therefore corresponds to a horizontal transport (in the direction of motion) of upper-layer water if the upper vortex is anticyclonic

(a 'warm heton') or lower-layer water if the upper vortex is cyclonic (a 'cold heton'). As is the case for the familiar barotropic vortex pair, propagation is in the direction that places the anticyclone on the right-hand side in the northern hemisphere, or the cyclone on the right in the southern hemisphere. In contrast, the class of vortex pairs consisting of vortices of opposite sign in the same layer carry density only when the two vortices have unequal strengths (giving unequal interface displacements), and then the pair can only move around a path of finite radius.

2.3. *Interactions of two vortex pairs*

Interactions between two or more baroclinic vortex pairs of the heton class were investigated by Hogg & Stommel (1985*a*) and Young (1985) through numerical integrations of the induced velocities (4). For example, a collection of two cyclonic vortices in one layer and two identical anticyclonic vortices in the opposite layer, but with all separation distances much greater than λ, gives rise to two hetons moving away from each other in opposite directions. While these appear, in plan view, to behave as two barotropic vortex pairs, the vortices of each pair are in opposite layers and the increasing separation of the pairs decreases the available potential energy of the system. If, on the other hand, the same four vortices are initially separated by distances of less than about one Rossby radius, the velocity shears across the interface associated with the baroclinic velocity distribution are sufficient to tear apart the upper- and lower-layer vortices making up each heton. In other words, interactions between vortices in the same layer are dominant over coupling through the interface. The two cyclones and two anticyclones simply cycle around their respective centres of vorticity in each layer and there is no change in available potential energy. In a reinterpretation of baroclinic instability Hogg & Stommel (1985*b*) used this example (but with a larger number of vortices) to show that a reduction of available potential energy can only be achieved efficiently by hetons having lengthscales d scaling with (but significantly larger than) the Rossby radius. Their results for the dominant lengthscale are in close agreement with those given by the classical stability analyses.

Numerical integrations for other configurations have shown that two vortex pairs of the heton type approaching each other along the same line can exchange partners to produce two new vortex pairs moving away at some angle to the original line of motion. Similarly, two hetons will repel each other, in a glancing collision, say, if the upper-layer component of each vortex pair has the same sign, or attract each other if the upper-layer component of each has opposite sign. Complex interactions such as these, though computed for ideal point vortices, may give some guide as to the structure and dynamics of individual interaction events in oceans and atmospheres.

3. Production of vortices in the laboratory

3.1. *Apparatus*

Experiments were carried out in a large circular tank 100 cm in diameter and 45 cm deep. This container was centred on the vertical axis of rotation of a rotating table. For all the experiments reported here, a rotation rate of 1.0 rad s^{-1} was used. The Plexiglas circular tank was surrounded by an outer square container and the intermediate space filled with water in order to facilitate undistorted horizontal views through the flow, revealing the density interface and motions of injected dye. Video and 35 mm cameras mounted above the tank and rotating with it enabled horizontal motions of floating particles, suspended neutrally buoyant particles and

injected dye to be monitored. A number of experiments were recorded on cine film, the remainder on video tape for later analysis. These visual records included a time scale in the form of a digital counter showing the number of tank revolutions (to $\frac{1}{10}$ of a revolution). One revolution period is 6.28 s.

Cyclonic vortices were generated by sinks at either the bottom of the tank or the free surface, and anticyclones by sources at the surface. Sinks on the bottom were holes 0.75 cm in diameter in a channel (0.5 cm high) laid on the base of the tank and leading to an outlet in the centre of the base. The angular position of the channel and the distance of holes from the centre could be adjusted. Sources and sinks at the free surface were short vertical tubes 3 cm in diameter filled with permeable plastic foam and intruding about 0.2 cm into the water (although the ends of small tubes 0.6 cm in diameter were also tried as sinks). The large diameter and presence of foam removed any jet-like behaviour for sources and yielded a uniform, laminar inflow. By passing connection tubes through rotating fluid couplings, sources and sinks were all controlled using flowmeters and valves in the non-rotating reference frame. Flow through the sinks was then driven by the head of water in the tank. Sources were supplied by gravity-driven flow from a reservoir of the same temperature and salinity as the upper layer. Small syringe tubing was fixed to the sources and sinks so that dye could be injected directly into the vortex cores.

Velocity fields associated with isolated vortices or with interacting vortices were obtained by directing a horizontal sheet of light 2 cm thick alternately through the mid-depth of the upper layer and the mid-depth of the lower layer in rapid succession. Long time exposures on high-contrast film revealed the paths of neutrally buoyant polystyrene beads (which had been added during the spin-up process). Photographs were generally taken three rotation periods apart, with alternate exposures showing particles in different layers.

3.2. *Two-layer stratification*

In order to create two layers of uniform density with the sharpest possible density step between them, a 20 cm deep layer of fresh water was first brought to solid-body rotation. A sugar solution of the desired density was then fed slowly on to the base through a tube near the wall. Once a more dense bottom layer reached a depth of 20 cm the inflow was stopped and the system left to approach solid-body rotation. The spin-up was monitored using the video camera, floating particles and dye motions. Internal Rossby radii used, based on the layer depth $H = 20$ cm and $f = 2\ \mathrm{s}^{-1}$, were 5, 10 and 15 cm.

While unstratified fluid always reached a state of no detectable motion, the two-layer system continued to experience persistent azimuthal motions for an indefinite time. This is the slow azimuthal drift noted by Griffiths & Linden (1985) and is believed to be the result of a meridional Eddington–Sweet circulation which, in turn, is driven by diffusion of solute across isopycnals. Hence the choice of sugar as solute in these experiments. The molecular-diffusion coefficient for sugar is one-third of that for salt, the more commonly used solute, and should minimize the magnitude of persistent motions. The motions were usually axisymmetric for the smaller density differences used (Rossby radii of 5 cm or less). For larger density differences the motions were of greater magnitude (close to 3 % of the rotation rate of the tank) and were often unstable and non-axisymmetric. Care was taken to begin experiments at times when the ambient motions were axisymmetric. Thus, although persistent motions were problematic, their influence on vortex motions was not great and can in most cases be taken into account.

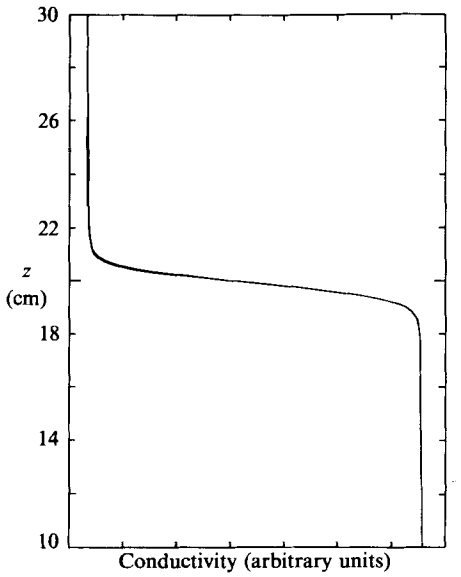

FIGURE 1. Two vertical profiles of conductivity through the same density interface before and after a typical experiment involving interaction of four vortices. The profiles begin and end at the mid-depth of each layer. They are so coincident as to be indistinguishable from each other. The overall density difference is 4.6% (using salt) giving $\lambda \approx 15$ cm. Density is nearly directly proportional to conductivity over this range. The interface is about 2 cm thick.

For completeness, density profiles were taken in a couple of experiments by traversing a conductivity probe along a vertical line. For these experiments it was necessary to use salt in place of sugar as the stratifying solute. The conductivity profiles, an example of which is shown in figure 1, show that 95% of the density change between layers occurs within an interfacial region 2 cm thick. A thinner interface cannot be obtained in such a large rotating container without resort to immiscible liquids, use of which poses other practical problems. It is difficult to obtain with immiscible liquids the small density differences required, and handling of noxious and volatile liquids can be a problem.

3.3. *Technique for generation of vortices*

Vortices were generated by turning on the flow through the desired sources and sinks. The flow rates were pre-set. Small amounts of dye were generally injected into the developing vortices, and dye was sometimes added to the incoming water for anticyclones. The flow was turned off after a fixed forcing period of 30 s, which is close to five rotation periods. Digital counters recording elapsed time in rotation periods were started from zero at the moment the forcing was turned off. Once the forcing was turned off vortices proceeded to interact freely with each other. The 30 s forcing period appeared to be sufficient to produce a well-developed vortex, independent of depth within its own layer. Injected dye formed vertical sheets in the horizontal shears of each vortex, along with nearly horizontal sheets in vertical shears at the density interface.

3.4. *Structure and strength of vortices*

Before investigating the interactions of laboratory vortices it is necessary to determine the velocity fields and vortex strengths established by the sources and

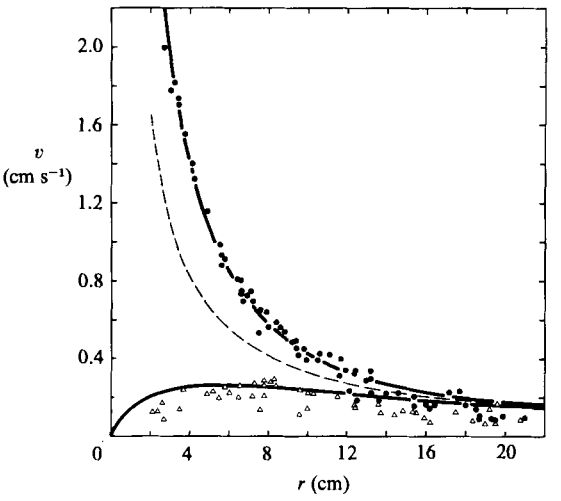

FIGURE 2. Measured azimuthal velocities in the upper layer (dots) and lower layer (triangles) for an isolated cyclonic vortex in the upper layer with $\lambda = 5$ cm. The measurements were taken from time exposures that began at 6 rotation periods (bottom layer) and 9 rotation periods (upper layer) after forcing ended. Solid curves are the profiles (3) predicted for point vortices. The fit to the upper-layer data gives the vortex intensity $s = 6.6$ cm^2 s^{-1}. The broken line is the reference curve $s/2r$ appropriate for barotropic vortices.

sinks. Figure 2 shows an example of the two-layer velocity distribution obtained from streak photographs of neutrally buoyant beads for a single isolated cyclone. The sink in this case was at the free surface. Streaklines near the vortex centre subscribed almost complete circles, and enabled the centre to be located to within 0.3 cm. Velocity profiles of the form (3) predicted for quasi-geostrophic point vortices provide a good description of the measured velocities in both layers in both cyclones and anticyclones, there being only one numerical constant, the vortex intensity s, to adjust in each case when fitting the theoretical curves. The measured lower-layer velocities in all vortices tested were smaller than those predicted, probably as a result of bottom friction and the finite interface thickness. Bottom friction, through Ekman pumping, will alter the potential vorticity in the bottom layer in proportion to the relative vorticity there, and therefore reduce the azimuthal velocity associated with a green upper-layer flow. An interface of finite thickness will reduce vertical velocity gradients in the interface and absorb some of the interface displacement required for geostrophic balance, thereby decreasing the relative vorticity induced by stretching or compression of columns in the lower layer.

A notable feature of the laboratory vortices is a core of finite radius within which the azimuthal velocity increases from $v = 0$ at $r = 0$ toward a maximum velocity at a radius of 3 or 4 cm. The absolute value of the angular velocity decreases monotonically at all radii and takes maximum values of 0.3Ω–0.5Ω in anticyclones, or 0.5Ω–1.0Ω in cyclones. With sinks, a strong vorticity concentration can be achieved, and this explains the higher values of initial angular velocity for cyclones. While the values of the initial Rossby number (0.3–0.5) of vortices of both signs seem rather large, the velocity profiles are closely predicted by the quasi-geostrophic model (see figure 2). However, the presence of a maximum velocity and finite core is a major departure from the point-vortex model, implying gradients of potential vorticity in the layer containing the vortex. The point-vortex model should give an accurate prediction of the trajectories of interacting vortices when the vortices

remain separated by distances much larger than the core radius. It will be seen in §4 that separations are not always large (because the core radius is not always much smaller than the Rossby radius, the influence of which we wish to investigate). The behaviour of interacting vortices can then be greatly altered by the presence of a finite core.

When simultaneously generating a number of vortices, it is essential to know their relative strengths. However, streak photographs which are needed for the determination of the vortex strength are less suitable for general visualisation of interacting vortices. It was therefore necessary to calibrate the sources and sinks by establishing a relationship between flow rate and vortex strength. Calibration required a separate set of runs in both two-layer and unstratified fills for which streak photography provided detailed velocity data. Profiles of the form of (3), or of the limiting form $v = \frac{1}{2}s/r$ for unstratified vortices, were fitted as in figure 2 in order to evaluate the vortex intensity s. Over the range of flow rates of interest, the vortex intensity was adequately represented as a linear function of the flow rate or, since the forcing time δt was fixed at 30 s, of the total volume injected or withdrawn (figure 3). However, a larger flow rate was required in order to generate a cyclone of the same strength as an anticyclone. Such a difference is not surprising given the much larger vorticity, and consequently larger dissipation, expected within the cores of cyclones during the forcing period. Note that the intensity of unstratified (barotropic) vortices is related to their circulation Γ by $s = \Gamma/\pi$. The vortex intensities plotted in figure 3 are those evaluated at a time 10 rotation periods after forcing was turned off. For all barotropic vortices, and baroclinic vortices in the bottom layer, bottom friction caused a spin-down over the timescale $H/(fv)^{\frac{1}{2}} \approx 140$ s. These vortices were generally followed for only 25–30 rotation periods. Baroclinic vortices in the upper layer spun down (or up) more slowly and could be followed for more than 50 rotation periods.

4. Vortex interactions in the laboratory

4.1. *Isolated hetons*

Single vortex pairs of the heton type were produced by placing a source at the free surface and a sink at the bottom of the fluid with a chosen horizontal separation d. Once the vortices had developed, the pair proceeded to move away slowly in the predicted direction. If the vortices were given different predetermined strengths, the pair moved along a strongly curved path, the weaker vortex turning around the stronger. These observations show that vortices in different layers influence each other. The individual hetons also served as an additional verification of the calibration of vortex intensities as a function of forcing parameters: trial-and-error adjustments of the flow rates until the vortex pair travelled through a distance of about $2d$ in a nearly straight line gave flow rates that were different for sources and sinks, but for which the calibration curves in figure 3 predict equal vortex strengths. On the other hand, all hetons eventually turned into a curved path, most probably as a result of the bottom-layer vortex spinning down due to bottom friction more rapidly than the top-layer vortex spun up due to a weak surface Ekman layer and horizontal diffusion of momentum. (Vortex Reynolds numbers based on the radius of maximum azimuthal velocity were close to 500.) The slow clockwise drift of the upper layer driven by the Eddington–Sweet circulation (§3.2) also contributed to the path curvature. In contrast, barotropic vortex created by the same source and sink in a single, unstratified layer continued along a straight line until they met the wall of the tank. The latter observation suggests that the beta-effect resulting from the

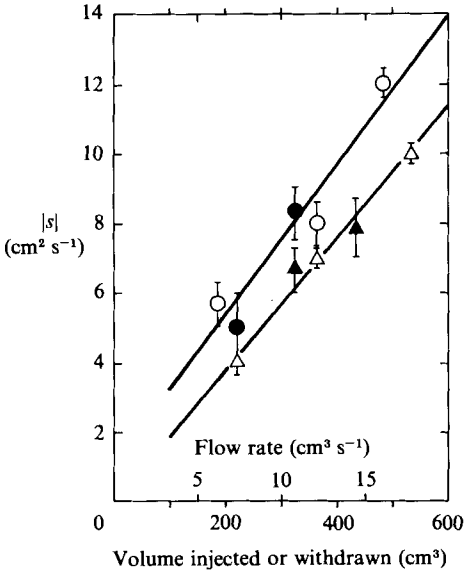

FIGURE 3. Vortex intensities s for a number of vortices produced by sources and sinks, as a function of the flow rate and total volume injected or withdrawn: △, barotropic cyclones: ▲, baroclinic cyclones with $\lambda = 5$ cm; ○, barotropic anticyclones; ●, baroclinic anticyclones with $\lambda = 5$ cm. The flow-rate calibration is valid for forcing over a period $\delta t = 30$ s. The solid lines are fitted by eye to the data for cyclones and anticyclones.

slope of the free surface relative to the bottom of the tank had little influence on the flow. The surface slope causes a vorticity change of about 1 % when the vortex is displaced by about 20 cm. Furthermore, the Rhines radius is of order 60 cm, which is much larger than the vortex spacings.

It is worthwhile pointing out explicitly that hetons with $d < \lambda$ translate more slowly than do baroclinic or barotropic vortex pairs with both vortices in the same layer. The small translation speed of hetons made measurements of the speed difficult to obtain in the time available before bottom-layer spin-down. However, when $\lambda = 5$ cm and both vortices were given initial intensities of $s \approx 6$ cm^2 s^{-1}, with separations in the range $5 < d < 15$ cm, the measured speed was in the range of 0.15–0.25 cm s^{-1}. This is in satisfactory agreement with the predicted speed (8) $c \approx 0.2$ cm s^{-1}, which is almost constant over the range of vortex separations used. Vortex pairs of the same strength in an unstratified layer moved somewhat more rapidly, as predicted, with $c \approx 0.5$ cm s^{-1} when $d = 5$ cm.

4.2. *Glancing collisions of two hetons*

Two similar hetons were generated in the configuration shown in figure 4. The two vortex pairs then moved toward each other along axes displaced by 14.8 cm, or three Rossby radii, and underwent a glancing collision. Within each pair, vortices of opposite sign in different layers were separated by $d = 1.3\lambda$. The paths traced out by the centres of the vortices (figure 4*a*) are similar to those expected of ideal point vortices (see figure 10*a* of Hogg & Stommel 1985*a*). Photographs in figure 4 (*b*, *c*) (Plate 1) show the vortex positions before and after collision. As the baroclinic vortex pairs approach each other, the anticyclones in the top layer come closer together than any other pair and interact strongly, inducing each other to move anticyclonically (clockwise) around their common centre of vorticity. This moves the anticyclones

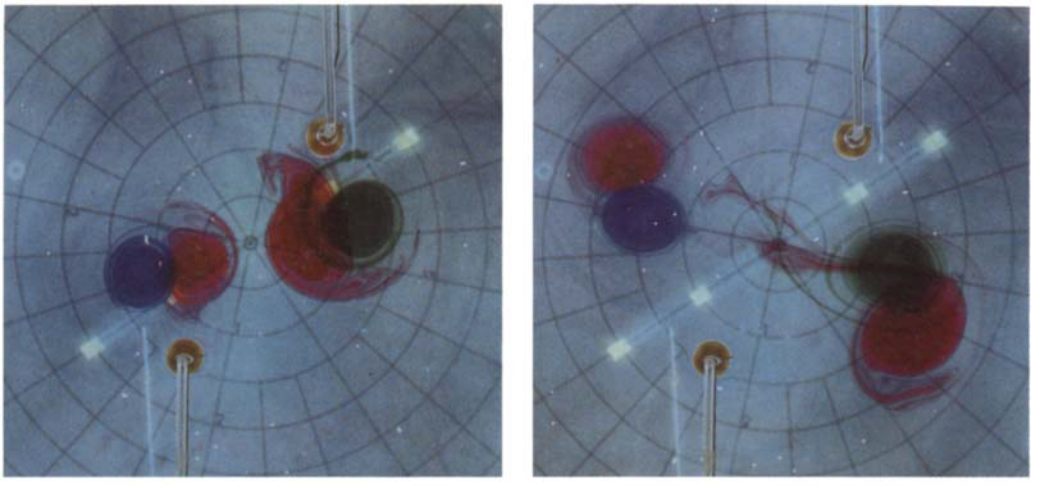

(b) *(c)*

FIGURE 4*(b,c)*. For caption see figure 4*(a)*.

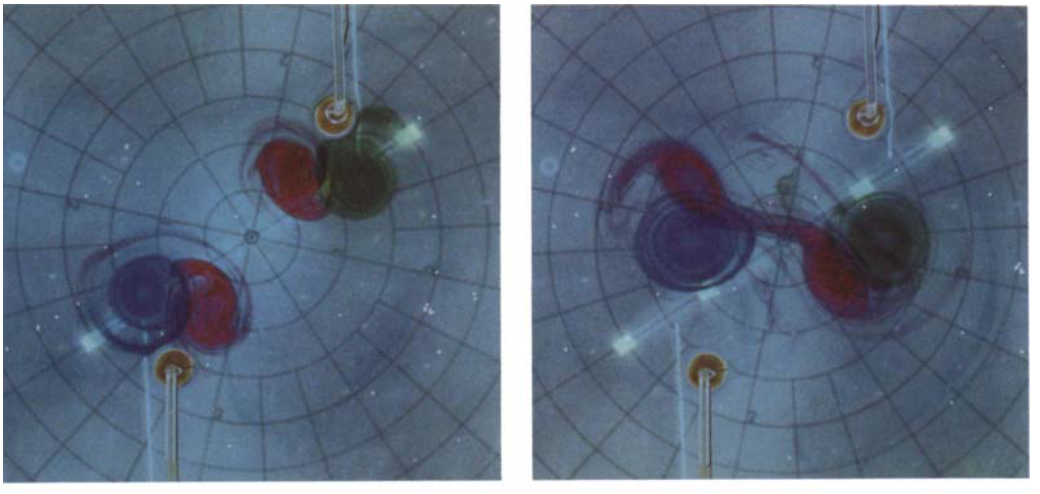

(a) *(b)*

FIGURE 5. Photographs of two stages during a very close glancing collision between like hetons similar to those of figure 4; $\lambda = 5$ cm, $s \approx 5.2$ cm^{2}s^{-1}. Photographs were taken at *(a)* $1.2T_\Omega$ and *(b)* $7.0T_\Omega$ after generation of the vortices. The two top-layer anticyclones (red dye) almost coalesce near $5T_\Omega$ but are pulled apart by the repelling vortex pairs.

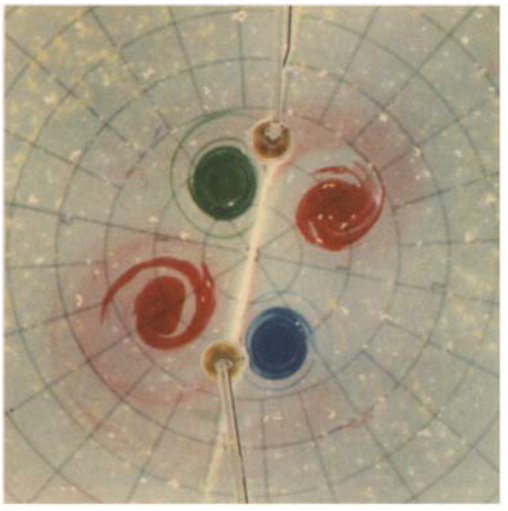

(b)

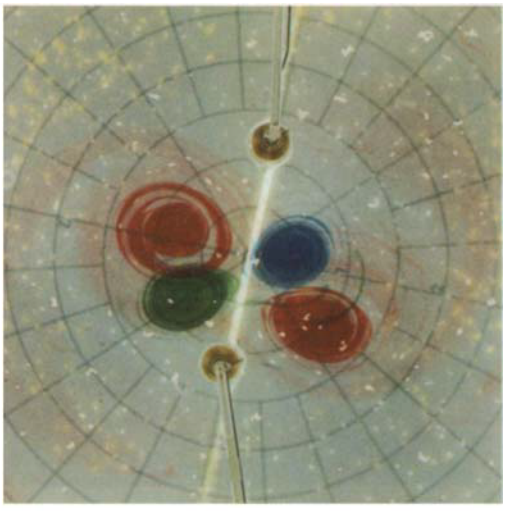

(c)

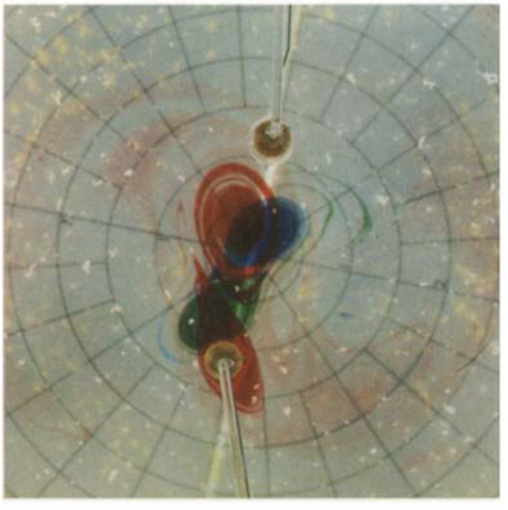

(d)

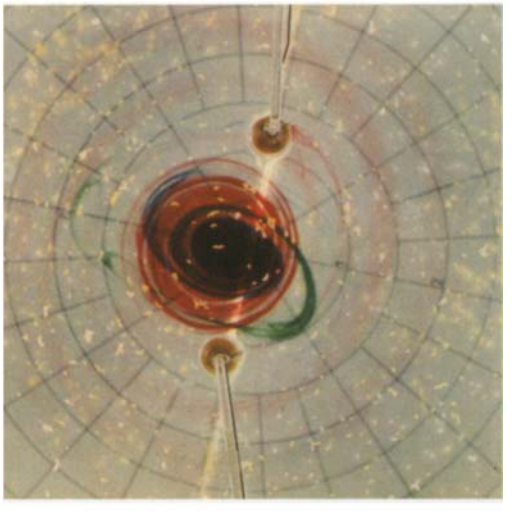

(e)

FIGURE 8*(b-e)*. For caption see figure 8*(a)*.

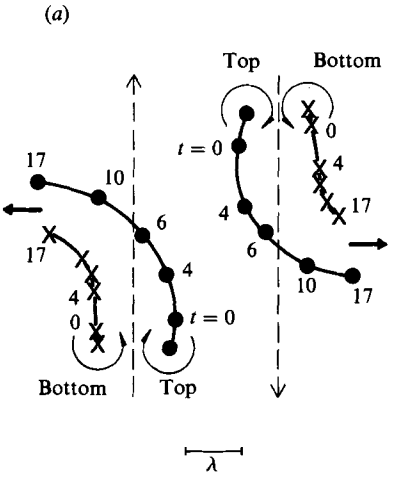

FIGURE 4. Two hetons in a glancing collision. Cyclones are in the bottom layer; anticyclones in the top layer. (*a*) shows the paths traced by the centre of each vortex. The times shown on the paths are in rotation periods $T_\Omega = 2\pi\Omega^{-1}$. Table rotation is anticlockwise; $\lambda = 5$ cm, $s \approx 5.2$ cm^2 s^{-1}. Vortices of opposite signs in each pair are separated by $d = 1.3\lambda$. Photographs in (*b*) and (*c*) (Plate 1) were taken at $t = 4.0T_\Omega$ and $10T_\Omega$, respectively. Red dye is in the top layer only; blue and green dyes in the bottom layer only. The dye does not show the size of the vortex cores, nor their strengths, but reveals the vortex positions and shapes. The vortex pairs repel. Vortex positions in photographs (*b*,*c*) are turned slightly clockwise with respect to traces in (*a*).

ahead of their accompanying cyclones (which tend to be held back by their tendency to move anticlockwise about their centre of vorticity), thereby steering the hetons into diverging paths. Thus the hetons repel each other.

Not all heton collisions are as straightforward as that described above. When the collision of figure 4 was repeated but with a smaller displacement between the axes (this time 1.8λ), the anticyclones were advected closer together by the heton translation. Near the point of closest approach the anticyclones, as revealed by dye in their cores, began to elongate and to wrap around each other. They almost coalesced but were eventually pulled apart by the influence of the cyclones. Photographs in figure 5 (Plate 1) show the dye in the vortices before, and just after, the collision, although simultaneous viewing of the shape and motion of dye and motion of floating particles are necessary to bring out the complexity of the interaction. The vortex pairs again repelled each other. However, it is felt that still more direct collisions of similar hetons may cause vortices of the same sign to merge together into a single vortex, a behaviour that is not allowed for in the point-vortex model. Even when coalescence does not occur, as in figure 5, the vortex paths deviate from those computed for point vortices and the heton paths are deflected through a smaller angle.

4.3. *A weakly symmetric collision*

In another form of collision, two hetons were generated in the weakly symmetric configuration shown in figure 6 and allowed to travel towards each other along a common axis. The separations of vortices within each vortex pair were altered, but in the example shown the separations were $d = 1.5\lambda$ and 3λ. As the pairs approach each other, the strongest interaction is between the anticyclone of one pair and the cyclone of the other pair. This interaction at a distance is predominantly between

(*a*)

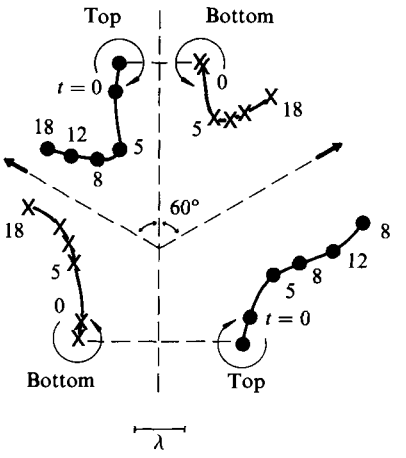

(*b*)

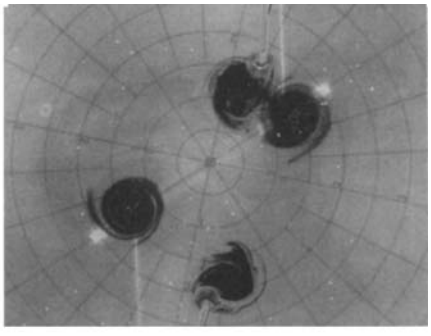

(*c*)

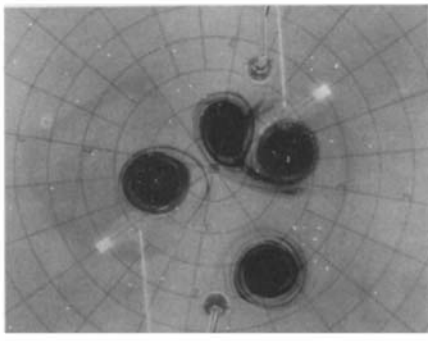

(*d*)

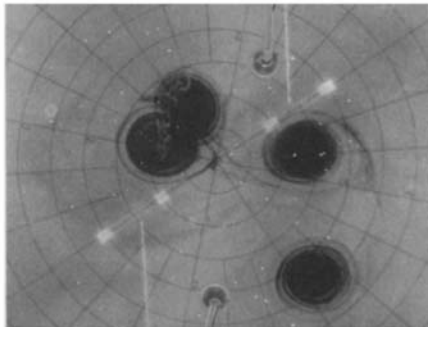

FIGURE 6. For caption see facing page.

barotropic velocity components, and dominates the collision. Vortices exchange partners to form two new hetons which travel away from each other. Photographs of the dyed vortices immediately after the forcing was turned of, near the point of closest approach and after closest approach, are shown in figure 6(*b–d*).

The paths in figure 6(*a*) are qualitatively similar to those computed by Young (1985) (his figure 10*a*). However, there are also effects of bottom friction: the bottom-layer cyclones spin down according to $s(t) = s(t_0)\exp[-(t-t_0)/140]$, where time is in seconds, while the top-layer anticyclones spin up much more slowly. In order to help overcome this problem† the cyclones were given initial strengths s_c slightly greater than the strength s_A of the anticyclones ($s_c \approx 7.5$ cm^2 s^{-1}, $s_A \approx 6.4$ cm^2 s^{-1}). The vortex strengths should have become equal at $t \gtrsim 3.5\,T_\Omega$, with the cyclones continuing to become weaker than the anticyclones at larger times. Thus vortices were of approximately equal strength as they entered the collision, with cyclones becoming relatively weak as the new hetons began to travel away. Another noticeable influence on the paths was the slow clockwise drift of the upper layer. This most affected the anticyclone at the bottom right which, as a result of the locations of the sources and sinks relative to the centre of the tank, was farther from the centre. The small relative velocity between layers has, of course, a cumulative effect on the vortex positions and interactions over time.

In other collisions with various vortex separations, and perhaps with small asymmetries in the initial conditions beyond our control, coalescence of vortices of like sign often occurred. Coalescence was more common in the lower layer, with the two cyclones merging into a single cyclonic vortex during the closest approach of the hetons. When the system was observed for very long times (over 50 rotation periods) the earlier merging of cyclones was often followed by merging of top-layer anticyclones. The difference between the layers might be traced to the asymmetry of dissipation in the two layers. We observed no 'slip-through' events in which vortices maintained their initial partnerships, one vortex pair passing through the other (Young 1985), as we did not attempt collisions with sufficiently small vortex separations within each heton.

4.4. *Repulsion of like hetons*

The weakly symmetric collision described above is dominated by the nearly barotropic far-field velocities induced by each vortex. The subsequent motion of similar vortex pairs along diverging paths can be described as the repulsion of like hetons. The increasing distance between hetons implies a decrease in the total potential energy of the flow (Hogg & Stommel 1985*a*). The likeness of hetons refers to the like-sign component vortices in the same layer. Thus two hetons having their anticyclonic

† Addition of a rigid lid in contact with the upper layer would have placed severe restrictions on our investigations. Addition of a much more dense third layer to reduce bottom friction induced stronger diffusion-driven flows and was abandoned.

FIGURE 6. The weakly symmetric collision between two hetons with $d = 7.5$ cm (upper pair) and $d = 15$ cm; $\lambda = 5$ cm. Vortex pairs are generated 27.7 cm apart (5.5λ). Cyclones are in the bottom layer and have initial strengths $s \approx 7.5$ cm^2 s^{-1}; anticyclones are in the top layer and have initial strengths $s \approx 6.4$ cm^2 s^{-1}. Vortex centres trace the paths shown in (*a*), where times are given in rotation periods T_Ω. Photographs in (*b–d*) were taken at $t = 0$, $8T_\Omega$ and $18T_\Omega$. Vortex pairs exchange partners and the new hetons repel. In all photographs, there is some parallax distortion as the top layer is closer to the camera than the bottom layer. The parallax is corrected in all diagrams. The vortex positions in the photographs (*b–d*) are turned clockwise with respect to traces in (*a*).

component in the top layer ('hot hetons'), or two hetons having their anticyclones in the bottom layer ('cold hetons'), repel each other. A 'hot heton' and a 'cold heton' attract each other. The repulsion can be demonstrated clearly by generating two cyclones in the bottom layer and two anticyclones in the top layer, each at a corner of a square or rectangle. Vortices must be separated by distances greater than about two Rossby radii. The subsequent motions of vortices are similar to those in the weakly symmetric collision of figure 6(*a*): interactions are predominantly barotropic, vortices influence their closest neighbours most strongly, and two like hetons move away in opposite directions.

Another interesting demonstration of heton repulsion is the behaviour of two hetons having no initial horizontal separation between the vortices of each pair ($d = 0$). We placed two sinks at the bottom 20 cm apart and a source at the surface directly above each sink. Two vortex pairs were generated, as shown in figure 7, the anticyclones directly above the cyclones with all vortices of equal strength. When the Rossby radius was 10 cm, the hetons were a distance 2λ apart. The barotropic components of the velocity field could not induce relative motion of the vortices, and initially there could be no motion of either heton. However, the baroclinic components of the velocities (3) caused interactions within each layer to be stronger than interactions across the interface. Cyclones therefore rotated a little in the anticlockwise sense, anticyclones a little in the clockwise sense, inducing a separation of the component vortices of each heton. This separation was in the correct sense to give the hetons finite translation velocities in opposite directions. The speed of translation was too small to measure accurately before dissipation influenced the vortex strengths, but was approximately 0.1 cm s^{-1}, consistent with that predicted by (8). The observed behaviour was in good agreement with that computed for point vortices (Hogg & Stommel 1985*a*, figure 8*b*), and reveals the weak baroclinicity of each vortex at distances greater than a Rossby radius. Further agreement with the point-vortex model was found when the Rossby radius was reduced to 5 cm, making the separation of source–sink pairs equal to 4λ. In that case the predicted final separation of cyclones and anticyclones and their translation speed were extremely small (see Hogg & Stommel 1985*a*, figure 8*a*), and indeed practically no relative motion of the vortices could be detected over 20 rotation periods.

4.5. *Splitting of hetons*

When the above experiment with two pairs of vertically stacked vortices placed 20 cm apart was repeated, but with a Rossby radius of 15 cm, two separate vortex pairs no longer emerged. Instead, the two top-layer anticyclones orbited around their centre of vorticity in the anticyclonic sense and the bottom-layer cyclones orbited about the same point but in the opposite direction, as shown in figures 8(*a*) and 8(*b–e*) (Plate 2). Vortices of opposite sign passed freely over each other with no obvious interaction through the density interface. In this case vortices are a distance 1.3λ apart and the experiment nicely reproduces the behaviour computed for corresponding point vortices when they lie less than a critical distances of 1.4λ apart (Hogg & Stommel 1985*a*, figure 8*c*). At these smaller distances the baroclinic components of the velocity field induced by each vortex dominate, giving a strong coupling between vortices in different layers. As a result, the total available potential energy (neglecting effects of dissipation) is conserved. This is in contrast to the release of available potential energy when the hetons of §4.4 repel each other. Only interactions over larger distances lead to a reduction of the potential energy of the flow.

The behaviour of the orbiting baroclinic vortices discussed above (and in many

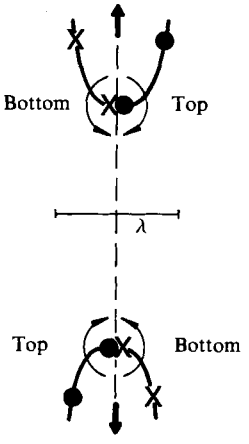

FIGURE 7. A diagrammatic representation of the paths traced by the centres of vortices when two hetons are generated with zero horizontal separation between vortices of opposite sign. Hetons are a distance 20 cm or 2λ apart; $\lambda = 10$ cm. Baroclinicity of the velocity fields causes the vortex pairs to repel.

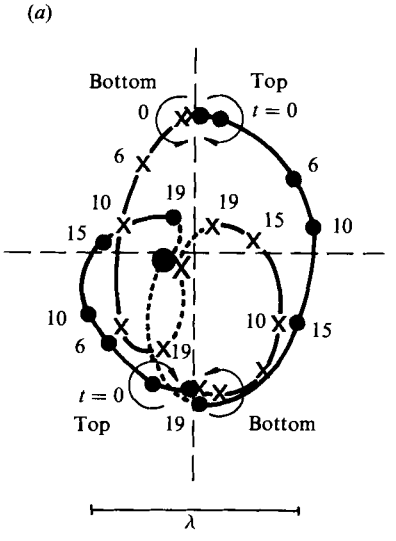

FIGURE 8. The behaviour of two pairs of vertically stacked vortices similar to those in figure 7, but this time pairs are a distance 20 cm or 1.3λ apart; $\lambda = 15$ cm, $s \approx 5$ cm^2 s^{-1}. The vortex centres trace the paths shown in (*a*). Photographs in (*b–e*) (Plate 2) were taken at times 6, 15, 22 and 45 rotation periods after generation of vortices. Red dye shows anticyclones in the top layer; blue and green dyes show cyclones in the bottom layer. Initial hetons are torn apart by baroclinic velocities, but like vortices coalesce and a single heton is formed. The vortex positions in the photographs (*b–e*) are turned slightly clockwise with respect to traces in (*a*).

similar experiments) eventually departed from that predicted by the point-vortex model. Vortices of like sign and in the same layer appeared to be particularly susceptible to non-ideal interactions leading to coalescence when they were separated by distances of the order of two Rossby radii or less. For example, in the experiment of figure 8, both top- and bottom-layer vortices began coalescing within 20 rotation periods (figure 8*c*), leaving only a single cyclone and a single anticyclone (a single heton) at 45 rotation periods (figure 8*d*).

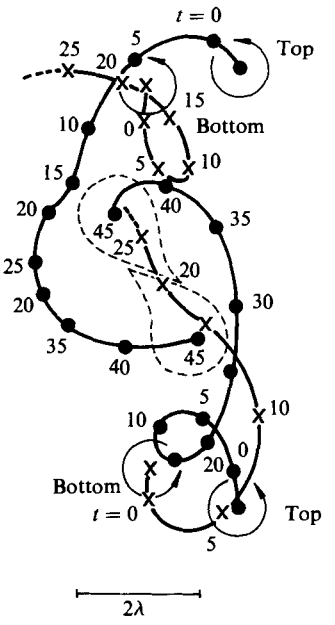

FIGURE 9. The paths traced by the centres of four cyclonic vortices, two in the top layer and two in the bottom layer; $\lambda = 5$ cm. Identical source and sink flow rates of 9.6 cm^3 s^{-1} gave vortex intensities $s \approx 5.6$ cm^2 s^{-1}. Early interactions are as for point vortices, but more complicated interactions and coalescing occur at later times.

4.6. *Coupling of vortices of like sign in different layers*

So far we have discussed only the interactions of vortices of opposite sign in different layers and of vortices of the same sign in the same layer. In both of these cases the vortices displace the density interface in the same direction and the total potential energy increases as the vortices are brought closer together. We therefore investigated the coupling of vortices of the same sign but in different layers. These vortices displace the interface in opposite directions and the available potential energy reaches a minimum when the two vortices lie directly above each other.

In figure 9 are shown the paths traced by four cyclonic vortices of identical initial strengths. These were generated as two pairs a large distance 6λ apart, each pair consisting of a cyclone in each layer a distance 1.3λ apart. The spinning of each pair clearly shows that the strongest coupling was that between the closest neighbours, even though these were in different layers. There was a weak long-range influence which coupled all four vortices and superimposed a slow anticlockwise motion about the centre of the array. For a period of about $10T_\Omega$ the paths were consistent with those computed for point sources (see Hogg & Stommel 1985*a*, figure 12*a*). After that period the trajectories began to deviate from those expected. By $20T_\Omega$ the two bottom-layer vortices were largely spun down. They were also drawn out and deformed by the influence of the top-layer cyclones as well as by interaction with each other until, after $25T_\Omega$, they were no longer well defined. In this and other experiments, it was not clear whether the deformation of bottom vortices by vortices of the same sign in a different layer could occur at any stage, or whether it only occurred after the bottom vortex had become very weak. In figure 9 the top-layer vortex C changed course at $15T_\Omega$ as a result of the influence of the approaching

bottom vortex B. Vortex C then continued to circle under the dominant influence first of B and later of the other top vortex A. Eventually, the two top vortices A and C were merely rotating around each other in close proximity. At $45T_\Omega$ these vortices developed cusps which were drawn out around the other vortex. The vortices quickly coalesced into one.

5. Conclusions

Laboratory experiments with geostrophic vortices in a two-layer stratification demonstrate fundamental interactions between baroclinic vortices. Of particular interest is the combination of two vortices of opposite sign in different layers, to which the name heton was recently given. The observed translation speeds of this class of vortex pair, and interactions between them, are for the most part consistent with the behaviour predicted by a simple model in which each vortex is modelled as a delta function in potential vorticity in one layer. Similar hetons tear each other apart over a distance of order one Rossby radius or less as a result of the velocity shears they induce across the interface. However, they repel each other if separated by larger distances. Thus the basic interactions between baroclinic vortices imply that the potential energy of the flow can be reduced only by motions with a sufficiently large lengthscale, relative to the Rossby radius.

Hogg & Stommel (1985*b*) further investigated the release of potential energy on the basis of numerical integrations of the spread of a large cloud of baroclinic point vortices. These computations showed that clumps of point vortices which emerged from the cloud took the form of distributed vortex pairs of the heton type, similar to structures that have been observed in experiments with unstable density fronts (Griffiths & Linden 1982). These clumps had a dominant lengthscale of 7.9λ. This lengthscale is similar to the dominant wavelength of unstable baroclinic waves predicted by classical quasi-geostrophic instability analyses (Pedlosky 1979) and observed in the experiments with unstable density fronts. Larger clumps were themselves unstable and broke up into smaller clumps. The vortex experiments reported in this paper do not give information about this dominant lengthscale, but rather demonstrate the basic mechanisms influencing the lengthscales on which potential energy can be released from a stratified, rotating flow.

Our experiments also reveal behaviour that is not predicted by modelling each laboratory vortex as a point vortex. The real vortices are characterized by finite areas of anomalous potential vorticity, and are observed to coalesce when vortices of like sign and in the same layer approach sufficiently close to each other. These vortices must be modelled as distributed clouds of baroclinic point vortices. The observed coalescing is, in appearance, similar to the pairing events for two-dimensional vortices in free shear layers (e.g. Brown & Roshko 1974) and to the merging in numerical simulations of two isolated finite-area vortices with cores of uniform vorticity (e.g. Christiansen & Zabusky 1973; Overman & Zabusky 1982; Aref 1983). However, the coalescing of baroclinic vortices of like sign involves the additional complication of potential-energy changes. Indeed, the coalescence must cause an *increase* in the total potential energy of the flow. Despite this, the numerical integrations of Hogg & Stommel (1985*b*) discussed above show clumping (or coalescing) of point vortices on scales sufficiently small for the newly formed clumps to be stable. The horizontal scales of coalescing vortices in the experiments too were significantly smaller than the scale 7.9λ. To this extent at least the observations are consistent with the model. However, little is known about the conditions necessary

for coalescence of real baroclinic vortices. The roles of the Rossby radius and internal vortex structure need to be examined. Coalescence is a problem of direct relevance to the interaction of geostrophic eddies (which have finite cores) in the ocean and atmosphere, and will be the subject of another article.

We express our appreciation of the invaluable assistance of Mr D. Corrigan in the laboratory and for the photographic expertise of Mr R. Wylde-Browne. E.J.H. thanks the Australian National University for the award of a Visiting Fellowship.

REFERENCES

AREF, H. 1983 Integrable, stochastic and turbulent vortex motion in two-dimensional flows. *Ann. Rev. Fluid Mech.* **15**, 345–389.

BROWN, G. L. & ROSHKO, A. 1974 On density effects and large structure in turbulent mixing layers. *J. Fluid Mech.* **64**, 775–816.

CHRISTIANSEN, J. P. & ZABUSKY, N. J. 1973 Instability, coalescence and fission of finite-area vortex structures. *J. Fluid Mech.* **61**, 219–243.

GRIFFITHS, R. W. & HOPFINGER, E. J. 1984 The structure of mesoscale turbulence and horizontal spreading at ocean fronts. *Deep-Sea Res.* **31**, 245–269.

GRIFFITHS, R. W. & LINDEN, P. F. 1982 Laboratory experiments on fronts. Part I: Density-driven boundary currents. *Geophys. Astrophys. Fluid Dyn.* **19**, 159–187.

GRIFFITHS, R. W. & LINDEN, P. F. 1985 Intermittent baroclinic instability and fluctuations in geophysical circulations. *Nature* **316**, 801–803.

GRYANIK, V. M. 1983 Dynamics of singular geostraphic vortices in a two-level model of the atmosphere (or ocean). (*Bull. Acad. Sci. USSR.*) *Atmos. Oceanic Phys.* **19**, 171–179.

HOGG, N. G. & STOMMEL, H. M. 1985*a* The heton, an elementary interaction between discrete baroclinic geostrophic vortices and its implications concerning eddy heat-flow. *Proc. R. Soc. Lond.* A **397**, 1–20.

HOGG, N. G. & STOMMEL, H. M. 1985*b* Hetonic explosions: the breakup and spread of warm pools as explained by baroclinic point vortices. *J. Atmos. Sci.* **42**, 1465–1476.

OVERMAN, E. A. & ZABUSKY, N. J. 1982 Evolution and merger of isolated vortex structures. *Phys. Fluids* **25**, 1297–1305.

PEDLOSKY, J. 1979 *Geophysical Fluid Dynamics.* Springer. 624 pp.

YOUNG, W. R. 1985 Some interactions between small numbers of baroclinic, geostrophic vortices. *Geophys. Astrophys. Fluid Dyn.* **33**, 35–61.